

Field Analysis of Shielded Uniaxial-Dielectric Rod Resonators

Y. Kobayashi and T. Senju

Department of Electrical and Electronical Engineering
Saitama University
Urawa, Saitama 338, Japan

Abstract — The rigorous field analysis by the mode matching method is presented for two dielectric rod resonators including such uniaxial-dielectrics as sapphire, which is placed between two parallel conducting plates and in a conducting cavity. The resonant frequencies of the some lowest modes are calculated. The validity is confirmed by experiment.

I. INTRODUCTION

Recently, sapphire dielectric resonators shielded by high Tc superconducting films have attracted special interest since they realize very high Q characteristic of over 2×10^6 below 90 K[1]. As is well known, single crystalline sapphires have relative permittivity perpendicular to the c-axis $\epsilon_t = 9.4$ and one parallel to the c-axis $\epsilon_z = 11.6$ because of their dielectric uniaxial anisotropy. Therefore, designing such resonators, we need to take account of the influence of anisotropic property on the resonant modes.

In this paper the rigorous field analysis by the mode matching method is described for shielded uniaxial-dielectric rod resonators of two types; parallel-plates and cavity-open types. The characteristic equations for these resonators are derived, the resonant frequencies of the some lowest modes are calculated, and mode charts are presented to design these resonators. The validity of theory is confirmed by experiment.

II. ANALYSIS

Fig. 1 shows two structures to be analyzed. One is parallel-plates type resonator shown in Fig. 1(a), where a dielectric rod is placed between two parallel, infinitely large conducting plates, and the other is cavity-open type resonator shown in Fig. 1(b), where a dielectric rod is placed symmetrically in a cylindrical conducting cavity.

In the field analysis discussed below we use a cylindrical coordinate system r, θ, z . The dielectric rod is assumed to be lossless homogeneous uniaxial anisotropic with the c-axis parallel to the z axis. Defining ϵ_t and ϵ_z as the relative permittivity perpendicular and parallel to the c-axis, respectively, the relative permittivity tensor $[\epsilon_r]$ is given by

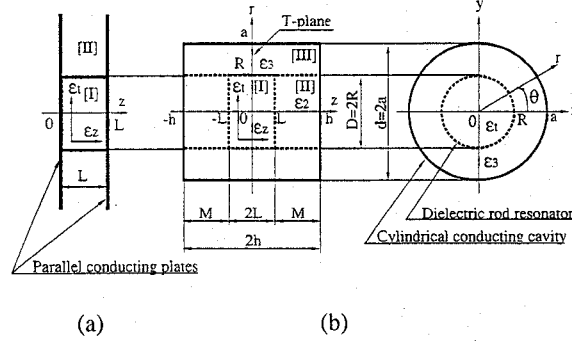


Fig. 1. Structures of shielded dielectric rod resonators.
(a) Parallel-plates type (b) Cavity-open type

$$[\epsilon_r] = \begin{bmatrix} \epsilon_t & 0 & 0 \\ 0 & \epsilon_t & 0 \\ 0 & 0 & \epsilon_z \end{bmatrix} \quad (1)$$

The relative permeability of the dielectric is assumed to be $\mu_r = 1$ and the conductor is also assumed to be lossless.

In a source-free condition and a time-harmonic factor $e^{j\omega t}$, Maxwell's equations can be written as follows:

$$\nabla \times \mathbf{E} = -j\omega \mu_0 \mathbf{H} \quad (2)$$

$$\nabla \times \mathbf{H} = j\omega \epsilon_0 [\epsilon_r] \mathbf{E} \quad (3)$$

$$\nabla \cdot [\epsilon_r] \mathbf{E} = 0 \quad (4)$$

$$\nabla \cdot \mathbf{H} = 0 \quad (5)$$

where \mathbf{E} and \mathbf{H} are the electric and magnetic fields, ϵ_0 and μ_0 are the permittivity and permeability of vacuum, respectively. Equation(4) can be rewritten as follows:

$$\nabla \cdot [\epsilon_r] \mathbf{E} = \epsilon_t \nabla \cdot \mathbf{E} - \epsilon_t \left(1 - \frac{\epsilon_z}{\epsilon_t}\right) \frac{\partial E_z}{\partial z} = 0 \quad (6)$$

Thus, we obtain

$$\nabla \cdot \mathbf{E} = \left(1 - \frac{\epsilon_z}{\epsilon_t}\right) \frac{\partial E_z}{\partial z} \quad (7)$$

Since the resonant modes in Fig. 1 are generally known to be hybrid, we then derive the wave equations for E_z and H_z .

OF2

Taking the rotation of (2) and using (3), we obtain

$$\nabla \times (\nabla \times \mathbf{E}) - k_0^2 [\epsilon_r] \mathbf{E} = 0 \quad (8)$$

where $k_0^2 = \omega^2 \epsilon_0 \mu_0$. Using the vector formula

$$(\nabla \cdot \nabla) \mathbf{E} = \nabla (\nabla \cdot \mathbf{E}) - \nabla \times (\nabla \times \mathbf{E}) \quad (9)$$

and (7), we obtain

$$(\nabla \cdot \nabla) \mathbf{E} - \left(1 - \frac{\epsilon_z}{\epsilon_t}\right) \nabla \left(\frac{\partial E_z}{\partial z} \right) + k_0^2 [\epsilon_r] \mathbf{E} = 0 \quad (10)$$

The z component of (10) yields the following wave equation for E_z :

$$\nabla^2 E_z - \left(1 - \frac{\epsilon_z}{\epsilon_t}\right) \frac{\partial^2 E_z}{\partial z^2} + \epsilon_z k_0^2 E_z = 0 \quad (11)$$

where ∇^2 is the Laplacian.

Similarly, taking the rotation of (3) and using (5) and (9), we obtain

$$(\nabla \cdot \nabla) \mathbf{H} + j \omega \epsilon_0 \nabla \times ([\epsilon_r] \mathbf{E}) = 0 \quad (12)$$

Using (2), we rewrite the second term of left side of (12) as follows:

$$\{ \nabla \times ([\epsilon_r] \mathbf{E}) \}_z = \epsilon_t (\nabla \times \mathbf{E})_z = -j \omega \mu_0 \epsilon_t H_z \quad (13)$$

The combination of the z component of (12) and (13) yields the following wave equation for H_z :

$$\nabla^2 H_z + \epsilon_t k_0^2 H_z = 0 \quad (14)$$

A. Parallel-Plates Type Resonator

We analyze the resonant modes for the structure shown in Fig. 1(a). Solutions of (11) and (14) are given by

$$E_{z1} = A_e J_n(k_{e1}r) \cos n\theta \cos \beta z \quad (15)$$

$$H_{z1} = A_m J_n(k_{m1}r) \sin n\theta \sin \beta z \quad (16)$$

for region [I] ($0 \leq r \leq R$) and

$$E_{z2} = B_e K_n(k'_2 r) \cos n\theta \cos \beta z \quad (17)$$

$$H_{z2} = B_m K_n(k'_2 r) \sin n\theta \sin \beta z \quad (18)$$

for region [II] ($r > R$) since $[\epsilon_r] = [1]$.

In the above,

$$k_{e1}^2 = \epsilon_z k_0^2 - \frac{\epsilon_z}{\epsilon_t} \beta^2 \quad k_{m1}^2 = \epsilon_t k_0^2 - \beta^2 \quad (19)$$

$$k'_2 = \beta^2 - k_0^2 \quad (20)$$

$$\beta = \frac{2\pi}{\lambda_g} = \frac{l\pi}{L} \quad ; l = 0, 1, 2, \dots \quad (21)$$

$$k_0 = \omega \sqrt{\epsilon_0 \mu_0} = \frac{2\pi}{\lambda_0} = \frac{2\pi f_0}{c} \quad (22)$$

and A_e , A_m , B_e , and B_m are constants determined from the boundary conditions. Also n and l denote the radial and axial mode numbers, respectively, β is the axial propagation constant, and $J_n(x)$ and $K_n(x)$ are the Bessel function of the first kind and the modified Bessel function of the second kind, respectively. The field components except E_z and H_z are given by substitution of (15)-(18) into (2) and (3).

The continuity of the tangential components of the electromagnetic fields between regions [I] and [II] yields the following characteristic equation for the hybrid modes:

$$\left[\epsilon_z \frac{J'_n(u_e)}{u_e J_n(u_e)} + \frac{K'_n(v)}{\sqrt{K_n(v)}} \right] \left[\frac{J'_n(u_m)}{u_m J_n(u_m)} + \frac{K'_n(v)}{\sqrt{K_n(v)}} \right] = \frac{n^2 \beta^2}{k_0^2} \left(\frac{1}{u_m^2} + \frac{1}{v^2} \right) \quad (23)$$

where $u_e = k_{e1}R$, $u_m = k_{m1}R$, and $v = k'_2 R$, the primes on $J_n(x)$ and $K_n(x)$ refer to differentiation with respect to their argument x . Equation (23) is different from one presented by Tobar et al.[2].

Particularly, when $n = 0$, (23) is divided into two for the TE_{0ml} and TM_{0ml} modes; that is,

$$\left[\frac{J'_0(u_m)}{u_m J_0(u_m)} + \frac{K'_0(v)}{\sqrt{K_0(v)}} \right] = 0 \quad (24)$$

for the TE_{0ml} modes and

$$\left[\epsilon_z \frac{J'_0(u_e)}{u_e J_0(u_e)} + \frac{K'_0(v)}{\sqrt{K_0(v)}} \right] = 0 \quad (25)$$

for the TM_{0ml} modes. Also, when $l = 0$, (23) yields

$$\left[\epsilon_z \frac{J'_n(u_e)}{u_e J_n(u_e)} + \frac{K'_n(v)}{\sqrt{K_n(v)}} \right] = 0 \quad (26)$$

for the leaky state TM_{nm0} modes[3].

B. Cavity-Open Type Resonator

The resonant modes for the structure shown in Fig. 1(b) can be rigorously analyzed by the mode matching method in a similar manner to the isotropic case, which has been already analyzed successfully[4]. The detail of analysis is omitted on account of the limited space. From the symmetry of the structure, the resonant modes are classified into ones where the T-plane ($r-\theta$ plane at $z = 0$) is an electric wall and the others where it is a magnetic wall. Thus, we consider only the $z \geq 0$ region, which is divided into three homogeneous subregions [I], [II], and [III]. The electromagnetic fields in each subregion are expanded in eigenmodes which satisfy the boundary conditions on the conductor surface and the T-plane. As a result, the resonant frequencies f_0 are determined from the condition that the following determinant vanishes:

$$\det H(f_0; \epsilon_t, \epsilon_z, \epsilon_2, \epsilon_3, D, 2L, d, 2h) = 0 \quad (27)$$

where matrix elements are omitted.

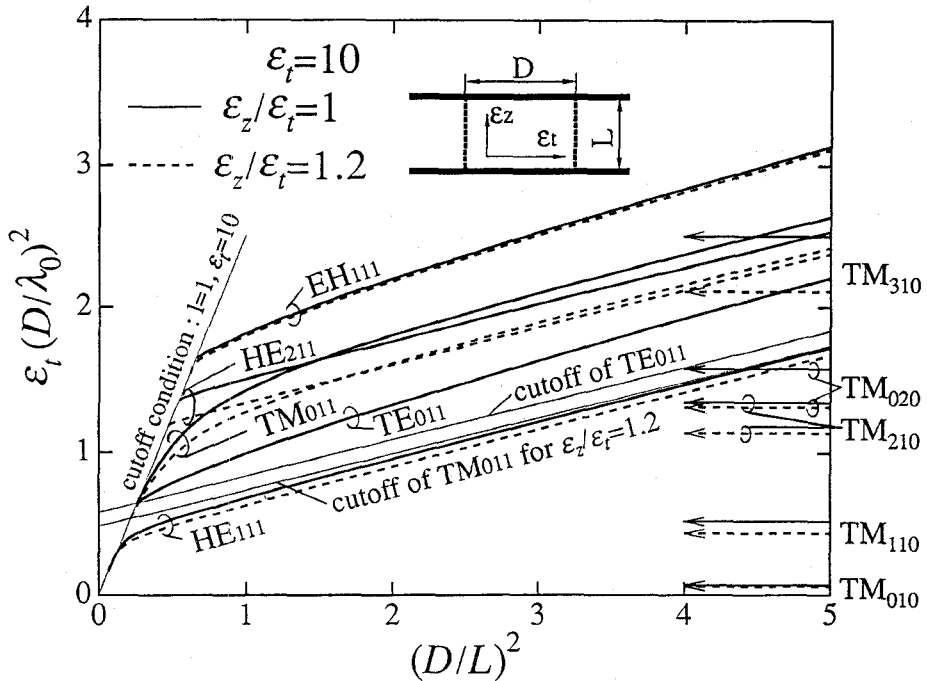


Fig. 2. Mode chart for a parallel-plates type resonator.

III. CALCULATIONS

A. Parallel-Plates Type Resonator

We can accurately compute the resonant frequencies for various modes by solving the corresponding transcendental equations (23)-(26) numerically. Fig. 2 shows a mode chart for the parallel-plates type resonator which is computed for the some lowest modes when $\epsilon_t = \epsilon_z = 10$ (solid curves) and when $\epsilon_t = 10$ and $\epsilon_z = 12$ (broken curves). The results calculated for the HE_{111} , TE_{011} , TM_{011} , and HE_{211} modes in the case of $\epsilon_t = 10$ and $\epsilon_z = 12$ show very good agreement with ones presented by Krupka[5] using the Galerkin-Rayleigh-Ritz method. The left side region of the cutoff condition in the figure indicates that the resonant modes are in a leaky state, where a part of the energy leaks away from the resonator in the radial direction[3]. The leaky state TM_{nm0} modes are independent of ϵ_z because they have only E_z components; thus, we can directly use the calculated values presented in [3]. The TE_{011} mode is independent of ϵ_z because it has no E_z component. The uniaxial property affects the resonant frequencies more strongly in the order, the TM_{011} , HE_{211} , HE_{111} , and EH_{111} modes according to the strength of the E_z component.

B. Cavity-Open Type Resonator

The resonant frequencies of the some lowest modes for the cavity-open type resonator were calculated from (27), where the size of the matrix for each resonant mode was taken so that the resonant frequency converge within 0.1 percent. The results are shown in Fig. 3 as a mode chart. The case of $\epsilon_t = \epsilon_z = 10$ is indicated by solid curves and the case of

$\epsilon_t = 10$ and $\epsilon_z = 12$ by broken curves. It is found that the uniaxial property of materials influences strongly on the resonant frequencies of the resonant modes having the predominant E_z component, such as the TM_{018} and HE_{118} modes, and weakly on ones having the predominant H_z component, such as the TE_{018} and EH_{118} modes. It is well known that the TE_{018} mode is dominant when $\epsilon_t = \epsilon_z$ is over 20 for the conventional dielectric resonators[4]. On the other hand, for sapphire resonators having relatively low permittivity about 10, the TM_{018} or EH_{118} mode become

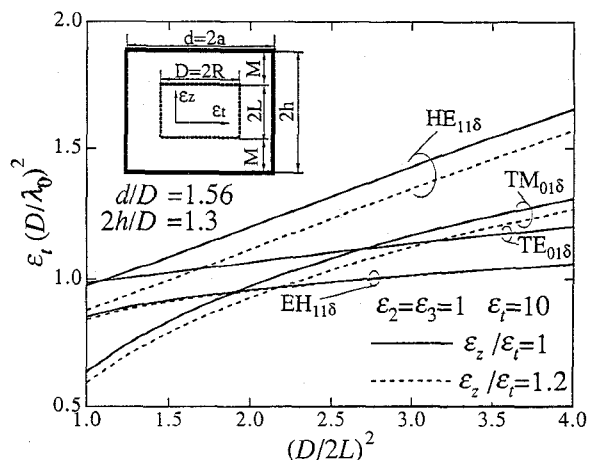


Fig. 3. Mode chart for a cavity-open type resonator.

dominant according as the dimension ratio $(D/2L)^2$ is smaller or greater than 2.

IV. EXPERIMENTS

The permittivity measurements were performed for two different samples of sapphire using the parallel-plates type resonator. The mode chart was used to identify the resonant modes for the different resonant frequencies. The results are shown in Table 1. The ϵ_t values were determined from the

Table 1. Measured values of ϵ_t and ϵ_z for sapphires.

Sample	D [mm]	L [mm]	f_0 [GHz]		ϵ_t	ϵ_z
			TE ₀₁₁	TM ₀₁₁		
1	9.985	9.998	9.739	10.948	9.393	11.479
2	10.002	5.002	13.550	14.272	9.400	11.615

measured resonant frequencies for the TE₀₁₁ mode by solving (24). Then we obtained the ϵ_z values from the measured resonant frequencies for the TM₀₁₁ mode and the ϵ_t values using (25). The values of ϵ_t and ϵ_z measured are in agreement within 1 percent with the published data.

To verify the validity of theory, experiments were performed for two cavity-open type resonators constructed by using the sapphires described above, a copper cavity having $d = 15.55$ mm and $2h = 13.00$ mm, and foamed plastic supports having $\epsilon_2 = 1.031$. The frequency responses of the transmission type resonators were measured using HP network analyzer. Two semirigid cables with small loops were used to excite and detect both the H_z and H_θ components of the fields. The results are shown in Fig. 4. The

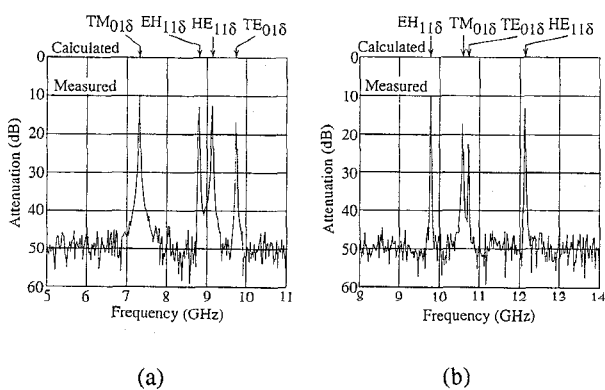


Fig. 4. Measured and calculated results of resonant frequencies for the lowest four modes ($d = 15.55$ mm, $2h = 13.00$ mm, $\epsilon_2 = 1.031$, $\epsilon_3 = 1$).

(a) $D = 9.985$ mm, $2L = 9.998$ mm, $\epsilon_t = 9.393$, $\epsilon_z = 11.479$
(b) $D = 10.002$ mm, $2L = 5.002$ mm, $\epsilon_t = 9.400$, $\epsilon_z = 11.615$

calculated values of resonant frequencies ($\epsilon_3 = 1$) are also indicated on the top of the figures. The agreement between theory and experiment is excellent.

V. CONCLUSIONS

The wave equations for E_z and H_z in a uniaxial anisotropic dielectric medium were derived under a cylindrical coordinate system. Based on these wave equations, the characteristic equations for two resonator structures were derived to calculate the resonant frequencies of any resonant modes. The mode charts useful to identify the resonant modes for sapphire rod resonators were presented. It was verified that the mode matching method used commonly for the analysis of isotropic-dielectric resonators can be applied successfully to that of uniaxial-dielectric resonators.

REFERENCES

- [1] Z. Y. Shen, C. Wilker, P. Pang, and W. Holstein, "High Tc superconductor-sapphire microwave resonator with extremely high Q-values up to 90 K," 1992 IEEE MTT-S Int. Microwave Symp. Dig., F-3, pp. 193-196.
- [2] M. E. Tobar and A. G. Mann, "Resonant frequencies of higher order modes in cylindrical anisotropic dielectric resonators," IEEE Trans. Microwave Theory Tech., vol. 39, pp. 2077-2082, Dec. 1991.
- [3] Y. Kobayashi and S. Tanaka, "Resonant modes of a dielectric rod resonator short-circuited at both ends by parallel conducting plates," IEEE Trans. Microwave Theory Tech., vol. MTT-28, pp. 1077-1085, Oct. 1980.
- [4] Y. Kobayashi, N. Fukuoka, and S. Yoshida, "Resonant modes for a shielded dielectric rod resonator," Electronics and Communication in Japan, vol. 64-B, no. 11, pp. 44-51, 1981.
- [5] J. Krupka, "Resonant modes in shielded cylindrical ferrite and single-crystal dielectric resonators," IEEE Trans. Microwave Theory Tech., vol. 37, pp. 691-697, Apr. 1989.